JOURNAL OF MATERIALS SCIENCE 30 (1995) 1473–1479

Dielectrical properties of u.v. cured acrylated polysiloxane films

L. M. LABORANTI, E. R. MOGNASCHI
Dipartimento di Fisica 'A Volta', Università di Pavia, via A. Bassi, 6-27100 Pavia, Italy
G. GOZZELINO, A. PRIOLA
Dipartimento di Scienza dei Materiali e Ingegneria Chimica, Politecnico di Torino, C. so Duca degli Abruzzi, 24-10129 Torino, Italy

The dielectric properties of films obtained through u.v. curing of an acrylated polysiloxane resin were evaluated in the temperature range from −136 to 24 °C. Different relaxation processes (α, β, γ, δ), characterized by decreasing dielectric relaxation intensities, were evidenced and quantitatively analysed: the α process was attributed to the glass transition process on the basis of the dynamic mechanical spectrum of the film and of its behaviour at different temperatures. The other processes (β, γ, δ), weaker than the α process, could be attributed to local dipolar motions present, even at low temperatures, in the polymer network.

1. Introduction

In the last years interesting structures of functionalized oligomers have become available. In particular different α–ω-diacrylates have been prepared which can give rise, after a curing reaction, to networks having specific properties and applications [1].

We use the u.v. curing technique for the bulk polymerization of the reactive oligomers; this technique is very suitable for obtaining complete and clear curing giving rise to polymeric networks with a well defined chemical structure [2]. The main applications of this technique are in the field of coatings, inks and in the electronic industry.

In this work we have considered an α–ω-diacrylated oligomer containing a polydimethylsiloxane segment linked at the ends to two poly-caprolactone segments. The oligomer was cured by u.v. curing technique; its relevance for applications is related to its use as an additive of u.v. curable coatings for modifying their properties.

Dielectric measurements as a function of temperature and frequency and mechanical and optical measurements as a function of temperature have been performed with the aim of characterizing the dynamic behaviour of this material.

2. Experimental procedure

2.1. Materials

As starting material an acrylated siloxane oligomer was used (80% solution in xylene), kindly supplied by BYK-Chemie (Wesel, Germany). The product is based on a polydimethylsiloxane having α,ω-hydroxypropyl groups. The OH-groups were esterified by ring opening reactions with caprolactone giving rise to a polyester modified polydimethylsiloxane. Afterwards the terminal OH-groups are reacted with isophoronediisocyanate resulting in an isocyanate functional preadduct. The two isocyanate groups are then reacted with hydroxylethyl acrylate resulting in a diacrylate functional polysiloxane adduct.

The structure of the obtained oligomer can be schematized as follows

$$R\text{–}[\text{–O–}(CH_2)_5\text{–CO–}]_6\text{–A–}(\text{–O–}\underset{\displaystyle CH_3}{\overset{\displaystyle CH_3}{\overset{|}{\underset{|}{Si}}}}\text{–})_{14}\text{–A–}[\text{–O–}(CH_2)_5\text{–CO–}]_6\text{–O–R}$$

where

$$A = \text{–}\underset{\displaystyle CH_3}{\overset{\displaystyle CH_3}{\overset{|}{\underset{|}{Si}}}}\text{–}(CH_2)_3\text{–O–},$$

$$R = CH_2{=}CH\text{–CO–O–}CH_2\text{–}CH_2\text{–O–CO–NH–R′–NH–CO–}$$

0022–2461

and R′ is the isophorone group. The average molecular weight $\bar{M}$ was 3200 ± 5%. The Si content of the resin was 12.5%, which corresponds to a 33.0% content of polysiloxane oligomer.

The added material of benzyldimethylketal (4 wt%) as photoinitiator was spread on a flat surface using the procedure previously reported [3, 4]. Films having thickness between 100 and 200 μm were obtained: they were u.v. irradiated under N_2 atmosphere until all the acrylic double bonds disappeared. The i.r. band at 1633 cm^{-1} was used for monitoring the acrylic double bond conversion which was found complete in any case. The films were colourless and transparent at room temperature indicating an homogeneous structure in agreement with dynamic–mechanical measurements. It was observed that the studied oligomer flows very slowly under constant stress yet exhibits elastic properties upon sharp impact.

2.2. Testing methods

For dielectric measurements a two-electrode condenser, made up by two rectangular copper electrodes of about 5 × 10 mm^2 with a rectangular sample cut from a leaf of the sample, 120 μm thick, inserted between them, was used. The light pressure exerted by an electrically insulated hairgrip held the two electrodes in place, providing the adherence of the sample to the electrodes and preventing the formation of an air layer between them and the sample. The choice of such a system was due to the fact that it was not possible to use silver paint electrodes, since chemical interaction between the paint solvents and the sample had been observed.

Two-electrode capacitance and conductance measurements of such a condenser, at different frequencies and temperatures, has been performed by means of a General Radio bridge model 1616, whose frequency range spans from 10 Hz to 100 kHz. The working voltage applied to the sample was about 0.5 V.

Because of the difficulties of evaluating the vacuum capacitance C_0 of the condenser, only values of capacitance C and conductance divided by the angular frequency G/ω will be reported in this work, instead of the real and imaginary part of the permittivity. However, the former are closely related to the latter by the following equations:

$$C(\omega) = \varepsilon'(\omega)C_0, \tag{1}$$

$$\frac{G(\omega)}{\omega} = \varepsilon'' C_0. \tag{2}$$

Preliminary measurements showed the existence of relaxation processes around and below room temperature, thus measurements at constant temperatures, over the whole frequency range of the bridge have been performed from about −136 °C to room temperatures. Unfortunately, at temperature above 0 °C the presence of d.c. conductivity, which affects conductance measurements in the low frequency region and whose contribution to $G(\omega)/\omega$ becomes more and more relevant as the temperature increases, makes measurements above room temperature less useful to the purpose of studying dielectric relaxations.

The dynamic–mechanical storage modulus E' and the mechanical loss tangent were measured, as a function of temperature from −50 °C to 150 °C with a Rheovibron instrument DDV-II at 110 Hz on a strip of the u.v. cured polymer. The size of the strip was 1.0 × 4.0 × 0.02 cm [3].

The refractive index n_D was measured at different temperatures, from about 12 °C to 70 °C with an accuracy of ± 0.0005 with an Abbe refractometer (Officine Galileo) illuminated by the yellow light of a sodium lamp. Technical difficulties prevented us performing measurements at lower temperatures.

3. Results and discussion

Fig. 1(a) and (b) report the values of G/ω versus frequency and Fig. 1(c) and (d) the values of C versus frequency at temperatures from −136 °C to 24 °C.

The main characteristic emerging from the graphs of Fig. 1 is the presence of multiple relaxation processes. In fact, the shapes of the plots of G/ω exhibit anomalous tails in the regions of lower and higher frequencies. This behaviour, which is typical of polymeric materials, can be interpreted by means of the superposition of two or more relaxation processes [5–7]. In the range of frequencies and temperature explored in our measurements four different relaxation processes were observed.

According to the generally accepted use the loss peak observed at the highest temperature (at a given frequency) or at the lowest frequency (at a given temperature) is defined as the α peak; β, γ, δ and following symbols are used to identify other relaxation processes in order of decreasing temperature or increasing frequency.

The analogous Cole–Cole plots, that is the graphs of G/ω versus C, not reported in this work, showed very flat arcs suggesting that also a distribution of relaxation times is present in each of the relaxation processes [5]. To fit the experimental data with a suitable function taking into account both the superposition of different relaxation processes and the distribution of relaxation times in each of them, we used a superposition of Cole–Cole-like equations [5] for $C(\omega)$ and $G(\omega)/\omega$ resulting in the following equations

$$C(\omega) = C_\infty + \sum_{i=1}^{N} \Delta C_i \times \frac{1 + (\omega\tau_i)^{1-\alpha_i}\sin(\tfrac{1}{2}\alpha_i\pi)}{1 + 2(\omega\tau_i)^{1-\alpha_i}\sin(\tfrac{1}{2}\alpha_i\pi) + (\omega\tau_i)^{2(1-\alpha_i)}} \tag{3}$$

$$\frac{G(\omega)}{\omega} = \sum_{i=1}^{N} \Delta C_i \times \frac{(\omega\tau_i)^{1-\alpha_i}\cos(\tfrac{1}{2}\alpha_i\pi)}{1 + 2(\omega\tau_i)^{1-\alpha_i}\sin(\tfrac{1}{2}\alpha_i\pi) + (\omega\tau_i)^{2(1-\alpha_i)}} \tag{4}$$

where N is the number of superposed relaxation processes observed at each temperature and α_i, τ_i and ΔC_i

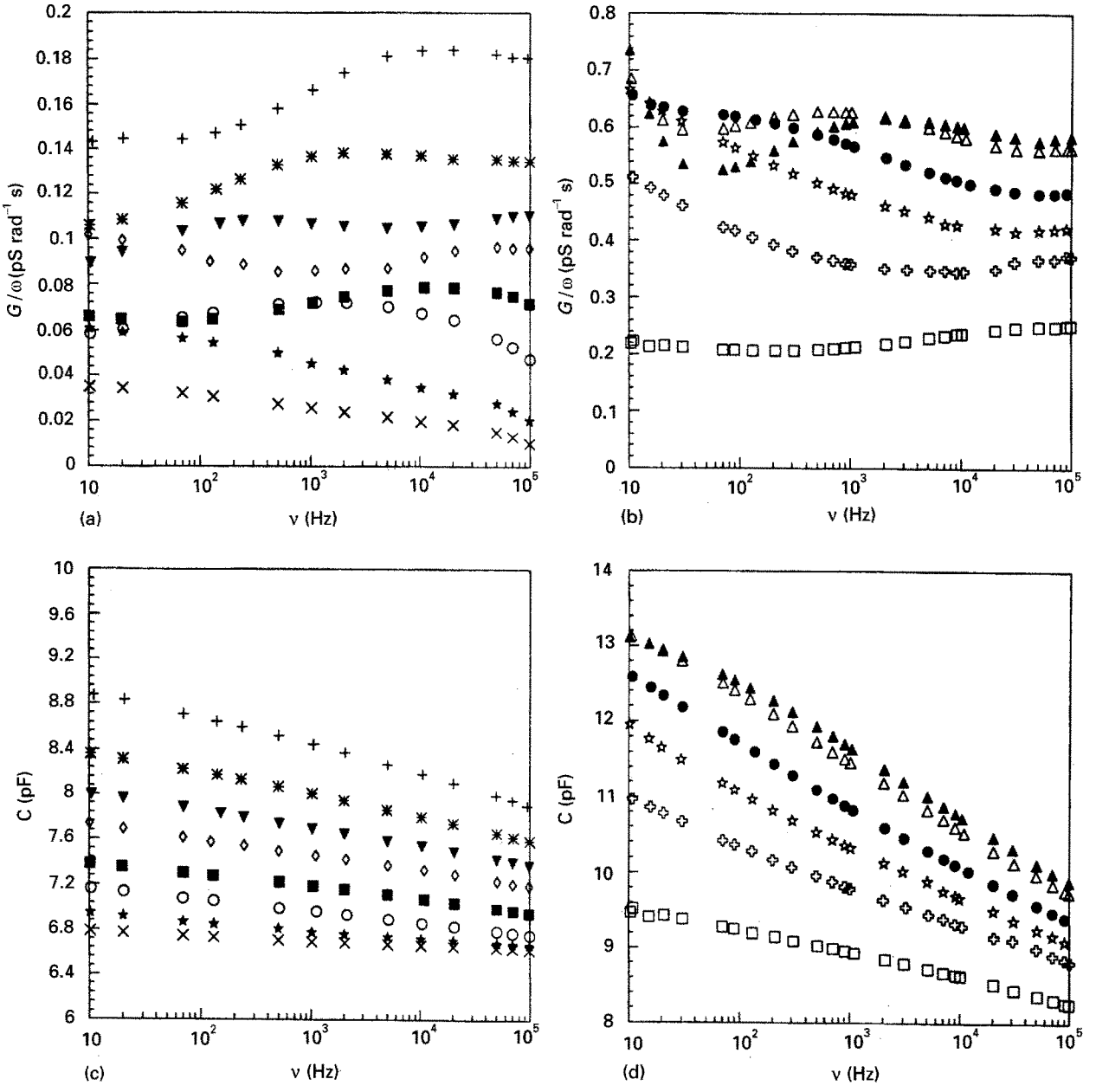

Figure 1 Experimental values of $G(\omega)/\omega$ in pS rad^{-1} s^{-1} (a) and (b), and of $C(\omega)$ (c) and (d), versus frequency ν, at different temperatures: (×) – 136.5 °C; (★) – 121.8 °C; (○) – 110.5 °C; (■) – 90.8 °C; (◇) – 70.3 °C; (▼) – 55.4 °C; (*) – 42.1 °C; (+) – 28.6 °C; (□) – 15.0 °C; (✠) 1.9 °C; (☆) 11.5 °C; (●) 17.8 °C; (△) 20.7 °C; (▲) 24.3 °C.

are, respectively, the Cole–Cole distribution parameter, the main relaxation time and the difference between the value of C at low and high frequencies for each relaxation process, and C_∞ is the high frequency capacitance.

The choice of a Cole–Cole function to account for the distribution of the relaxation times is mainly due to its relatively simple mathematical expression and, moreover, because there was no relevant reason leading to the use of a different approach, for example, a particular asymmetry in the Cole–Cole arcs.

The fitting procedure has been performed by first analysing the plot of $G(\omega)/\omega$ versus frequency at each temperature by means of Equation 4, determining from this analysis the best values for the parameters α_i, τ_i and ΔC_i, and then using these values to determine the best value of C_∞ fitting the experimental data of $C(\omega)$ by means of Equation 3. This procedure takes into account . that $C(\omega)$ and $G(\omega)/\omega$ are related through the equivalent of Krönig–Kramers relations and, therefore, the set of parameters α_i, τ_i and ΔC_i must be the same for both $G(\omega)/\omega$ and $C(\omega)$ at a given temperature.

At temperatures above 0 °C, as already mentioned, we had to consider also the presence of d.c. conductivity affecting the measurements of $G(\omega)/\omega$ in the low frequency region. To take into account this effect, when present, a term inversely proportional to ω has been added to the expression of $G(\omega)/\omega$ so that Equation 4 becomes

$$\frac{G(\omega)}{\omega} = \frac{K}{\omega} + \sum_{i=1}^{N} \Delta C_i \times \frac{(\omega\tau_i)^{1-\alpha_i}\cos(\frac{1}{2}\alpha_i\pi)}{1 + 2(\omega\tau_i)^{1-\alpha_i}\sin(\frac{1}{2}\alpha_i\pi) + (\omega\tau_i)^{2(1-\alpha_i)}} \quad (5)$$

where K is the temperature-dependent d.c. conductance.

TABLE I Values of the parameters ΔC_i in pF, α_i and τ_i in s, for the different relaxation processes, together with K and C_∞ at different temperatures, obtained from the best fits of experimental data using the superposition of Cole–Cole-like functions

T °C	Relaxation process					K (pS)	C_∞ (pF)
		α	β	γ	δ		
− 136.5	ΔC_i			0.27	0.03		
	α_i			0.69	0.39		6.62
	τ_i			1.57×10^{-2}	1.47×10^{-5}		
− 121.8	ΔC_i		1.02	0.41	0.04		
	α_i		0.73	0.69	0.41		6.64
	τ_i		1.13×10^{4}	5.54×10^{-3}	9.39×10^{-6}		
− 110.5	ΔC_i		0.94	0.50	0.05		
	α_i		0.73	0.69	0.34		6.67
	τ_i		1.11×10^{3}	2.13×10^{-4}	6.74×10^{-6}		
− 90.8	ΔC_i		0.84	0.47	0.05		
	α_i		0.74	0.66	0.49		6.76
	τ_i		6.70	1.02×10^{-5}	4.40×10^{-7}		
− 70.3	ΔC_i		0.85	0.54			
	α_i		0.72	0.63			6.86
	τ_i		5.70×10^{-2}	9.91×10^{-7}			
− 55.4	ΔC_i		0.87	0.56			
	α_i		0.72	0.61			6.84
	τ_i		1.16×10^{-3}	1.07×10^{-7}			
− 42.1	ΔC_i	5.39	0.96	0.58			
	α_i	0.73	0.71	0.63			6.90
	τ_i	5.60×10^{4}	9.53×10^{-5}	3.39×10^{-8}			
− 28.6	ΔC_i	5.65	1.39	0.53			
	α_i	0.75	0.72	0.63			6.90
	τ_i	4.96×10^{3}	9.53×10^{-6}	3.19×10^{-9}			
− 15.0	ΔC_i	5.62	2.24	0.53			
	α_i	0.76	0.76	0.63			6.53
	τ_i	3.97×10^{2}	1.21×10^{-6}	1.07×10^{-9}			
1.9	ΔC_i	5.76	2.81				
	α_i	0.76	0.71			1.51	6.61
	τ_i	5.84×10^{-1}	1.23×10^{-7}				
11.5	ΔC_i	5.82	2.79				
	α_i	0.75	0.70			4.60	6.51
	τ_i	2.90×10^{-2}	4.92×10^{-8}				
17.8	ΔC_i	5.85	2.86				
	α_i	0.75	0.66			5.05	6.30
	τ_i	3.47×10^{-3}	2.15×10^{-8}				
20.7	ΔC_i	5.74	3.04				
	α_i	0.74	0.57			14.39	5.88
	τ_i	3.07×10^{-4}	9.85×10^{-9}				
24.3	ΔC_i	5.52	3.28				
	α_i	0.73	0.47			23.82	5.28
	τ_i	6.48×10^{-5}	9.85×10^{-9}				

In Table I the values of the parameters ΔC_i, α_i and τ_i obtained from the best fits are reported together with K, when present, and C_∞. The four different relaxation processes observed were labelled α, β, γ and δ in order of decreasing temperature; they are characterized by decreasing dielectric relaxation intensities in the same order.

We have to emphasize that at each temperature only two or three relaxation processes, among α, β, γ and δ, give a significant contribution to the relaxation spectrum. At higher temperatures only the α and β processes were considered since the tails of the γ and δ processes were negligible. Below 0 °C the third relaxation process γ became relevant, while below −40 °C the α process contribution became, in turn, negligible. At −90 °C the fourth relaxation process δ became observable and, finally, at the lowest temperatures only the γ and δ relaxation processes were taken into account.

From the results of our analysis, we can observe that the investigated films show a main relaxation process α which exhibits maxima of $G(\omega)/\omega$ in the frequency range of our measurement system at about room temperature, although partially hidden by the rise of d.c. conductivity with the rise of temperature, as one can see from Fig. 1b.

Correspondingly, dynamic–mechanical measurements at 110 Hz, reported in Fig. 2, show a decrease of several orders of magnitude of the elastic modulus, associated with a peak of the mechanical tan δ with the maximum at about 23 °C.

Fig. 3 reports the refractivity values of the cured film, defined as $n_D - 1$, as a function of temperature. A best fit of experimental data with a single straight line shows that some points are far from this line by more than the standard deviation. For this reason the temperature range has been divided into three

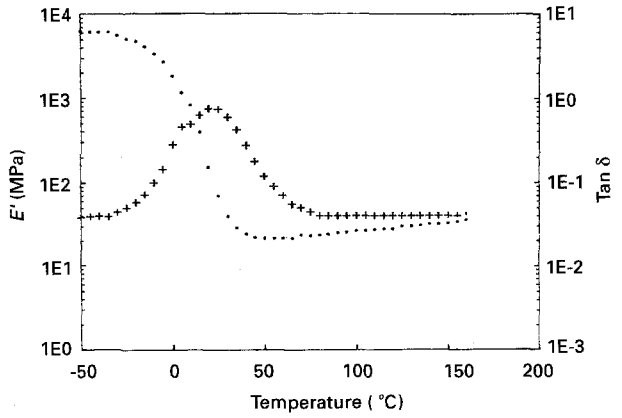

Figure 2 Mechanical elastic modulus E' (●) and loss tangent $\tan\delta$(+) versus temperature at 110 Hz.

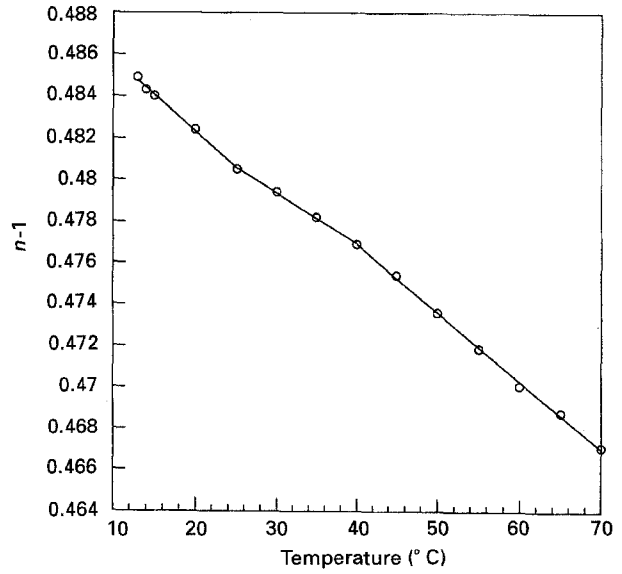

Figure 3 Refractivity data versus temperature.

consecutive intervals and the experimental points in each of them have been fitted by means of different straight lines. The equation for each line is

$$n_D - 1 = AT + B \qquad (6)$$

where T is the temperature in degrees centigrade and $A = dn_D/dT$ represents the thermo-optic coefficient of the material [8]. The best fit procedure gives: in the temperature range from 12 °C to 22 °C: $A = -3.51 \times 10^{-4}\,°C^{-1}$, $B = 0.4893$; from 22 °C to 38 °C: $A = -2.41 \times 10^{-4}\,°C^{-1}$, $B = 0.4866$; from 38 °C to 70 °C: $A = -3.29 \times 10^{-4}\,°C^{-1}$, $B = 0.4901$. In Fig. 3 segments of the three best fit straight lines are also shown. The first change of dn_D/dT could be assigned to the α transition in agreement with the results of dynamic–mechanical measurements. No explanation at the moment are possible for the second variation of dn_D/dT at about 40 °C, although this variation of the thermo-optic coefficient could be related to a subtle structural transition not detected by dielectric or mechanical measurements.

A secondary relaxation process β presents dielectric loss peaks with maxima in our frequency range at temperatures between −28 °C and −70 °C. These peaks are characterized by a narrower distribution of relaxation times with respect to those of the α process, but their height, evaluated by the expression [5]

$$\left(\frac{G(\omega)}{\omega}\right)_{max} = \frac{1}{2}\Delta C_i \frac{\cos(\alpha_i(\pi/2))}{1 + \sin(\alpha_i \pi/2)}, \qquad (7)$$

increases with increasing temperature, while the height of the peaks of the α process remain roughly constant.

For temperatures below −70 °C and above −130 °C the γ and δ processes show loss peaks in the explored frequency range. Their characteristic broadness and height are less relevant than those of the previous processes, but their presence reveals the existence of dipolar motions in the polymer chain even at low temperature.

In Fig. 4 two of the most significative graphs are presented in which, beside the experimental points, the fitting curve together with the curve representing each process taking part to the superposition of relaxation in process are drawn. In Fig. 4b, which represents data at the highest temperature, the contribution of d.c. conductivity is also drawn.

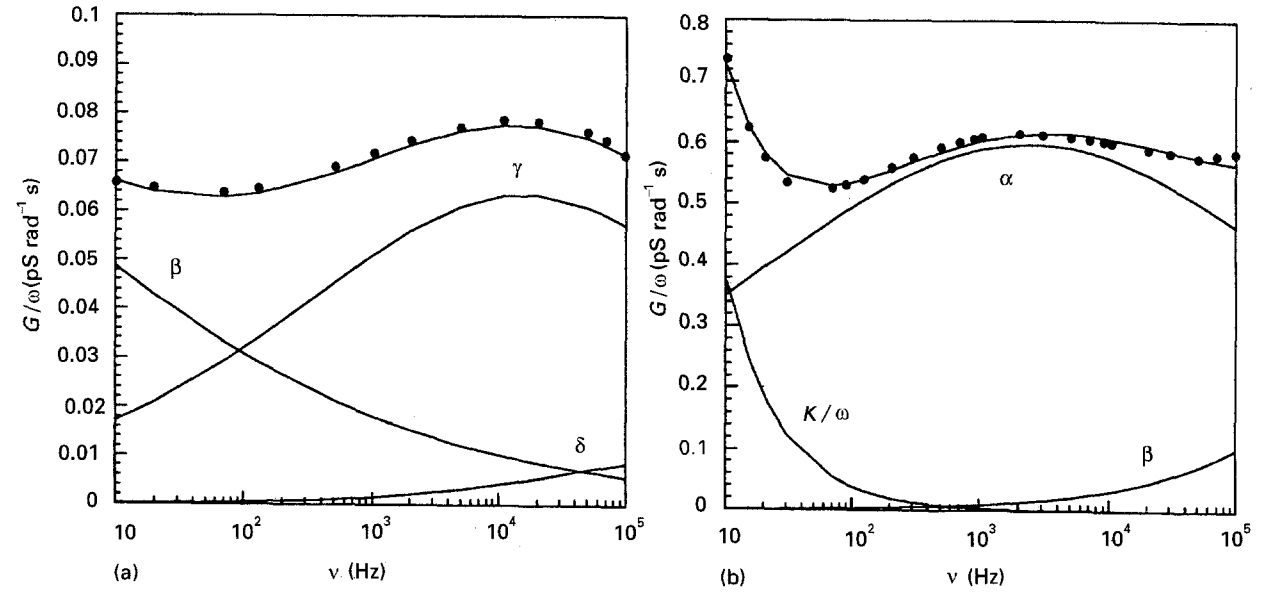

Figure 4 Experimental points of $G(\omega)/\omega$ versus frequency and fitting curves: (a) at −90.8 °C and (b) at −24.3 °C.

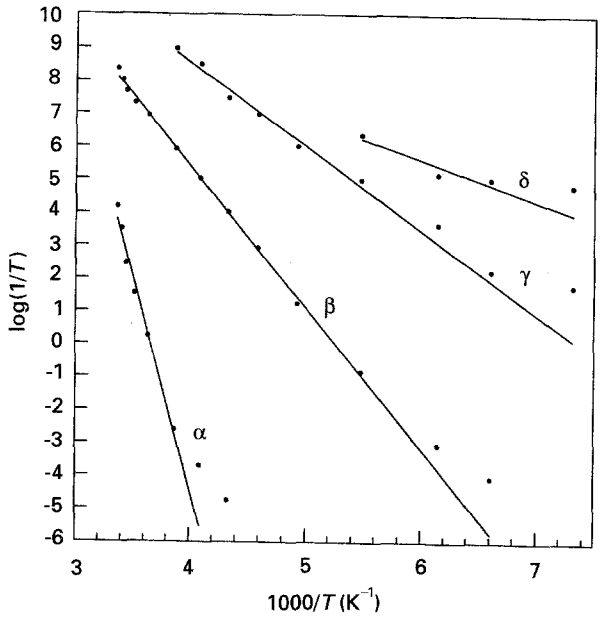

Figure 5 Inverse of dielectric relaxation times versus $1000/T$ for the four observed relaxation processes.

The inverse of the dielectric relaxation times, i.e. the relaxation rates determined through the best fits of experimental results are plotted in a semilogarithmic graph versus $1000/T$ in Fig. 5, where T is the absolute temperature in °K. The relaxation rates of the four relaxation processes found in our analysis are distributed along four curves. The high temperature parts of such curves exhibit a linear behaviour whose slopes represent the apparent activation energy of each process according to the law

$$\frac{1}{\tau} = \frac{1}{\tau_0} \exp\left(\frac{-E_A}{kT}\right) \tag{8}$$

in which τ_0 is a proportionality constant, k is the Boltzman constant, and E_A is the activation energy.

By fitting the experimental points in the graph of Fig. 5, we obtained the values of E_A which are: 25.0 kcal mol^{-1} for the α process, 8.3 kcal mol^{-1} for the β process, 5.0 kcal mol^{-1} for the γ process and 3.5 kcal mol^{-1} for the δ process.

4. Conclusions

For polymers in the amorphous state a relaxation region is observed at temperatures around and above the glass transition temperature T_g. This relaxation is usually labelled α and is referred to as the primary or glass–rubber relaxation [6]. It is frequently the most prominent dielectric loss peak and it is characterized by an amplitude slowly varying with temperature, while the β peaks appear relatively broader with respect to the α peaks and their amplitude decreases with decreasing temperature.

The investigation of the dielectric, mechanical and optical properties of the u.v. cured acrylated polysiloxane films, evidenced different relaxation processes. The relaxation process observed at the highest temperature was attributed to the α process either because of the typical behaviour of the relaxation process itself at different temperatures and because the dynamic–mechanical measurements show a relevant decrease of the elastic modulus in the same temperature range (Fig. 2). In fact, as we can see from the data of Table I and by means of Equation 7, the amplitude of the α peak remains roughly constant at different temperatures, while that of β peaks increases with increasing temperature.

We can observe the high value of T_g presented by the investigated system (about 23 °C) with respect to the T_g values of poly-dimethylsiloxane (− 127 °C) [9] and of poly-caprolactone (− 64 °C) [10]. The presence of the acrylic and particularly of the rigid urethane structures can explain the high increase in the T_g value.

As far as the other low temperature relaxation processes are concerned, they can be attributed to dipolar motions present in the system even at low temperatures. Usually, to account for secondary relaxations, torsional oscillations and local conformational transitions of the skeletal bonds, crankshaft and kink motion and motion of side groups are invoked [11]. It is impossible at the moment to attribute these relaxation processes to a particular polar group motion, due to the complexity of the molecule. In fact, in the investigated system many different structures are present, namely polysiloxane, polyether, ester and urethane structures which could give rise to different relaxation processes. However, these relaxations can be attributed to restricted local motions in the material which do not influence the mechanical properties, at least to − 50 °C as we can see from the dynamic–mechanical spectrum of the material. Recent studies devoted to explain the weak β absorptions of some model compounds of polyacrylates at the molecular level [12] suggested that intermolecular interactions must play an important role in the origin of such relaxation processes.

The temperature dependence of the refractive index is characterized by thermo-optical coefficients with values typical of organic compounds and, in particular, of polymers [13]. The existence of temperature regions with different thermo-optical coefficients can be due to structural transition phenomena which could take place in the polysiloxane film studied. Furthermore, it is to be noted that in correspondence with the temperatures at which a change in the thermo-optical coefficient occurred, the dielectric and mechanical measurement revealed the existence of the glass transition.

Acknowledgements

We thank BYK-Chemie G.m.b.H. for kindly supplying the polysiloxane resin (LP-G-5834) and acknowledge the Italian CNR (Chimica Fine II Finalized Project) and MURST for financial support through the Instituto Nazionale di Fisica della Materia.

References

1. C. E. HOYLE and S. F. KINSTLE (eds.), "Radiation Curing of Polymeric Materials", ACS Symposium, Series No. 417, Washington (1990).

2. A. PRIOLA, G. GOZZELINO, F. FERRERO and G. MALUCELLI, *Polymer* **34** (1993) 3653.
3. A. PRIOLA and F. RENZI, *J. Mater. Sci.* **20** (1985) 2885.
4. A. PRIOLA, G. GOZZELINO and F. FERRERO, *Int. J. Adhesion Adhesives* **10** (1990) 77.
5. C. J. F. BÖTTCHER and P. BORDEWIJK, Theory of electric polarisation, vol. II (Elsevier, Amsterdam, 1978).
6. N. G. Mc CRUM, B. E. READ and G. WILLIAMS, "Anelastic and dielectric effects in polymeric solids" (John Wiley & Sons, London, 1967).
7. A. K. JONSCHER, "Dielectric relaxation in solids" (Chelsea Dielectric Press, London, 1983).
8. H. J. HOFFMANN, *J. Phys. IV (France)* **2** (1992) C2–21.
9. U. GAUR, S. F. LAU and B. WUNDERLICH, *J. Phys. Chem.* **12** (1983) 91.
10. *Idem., ibid.* **12** (1983) 65.
11. R. H. BOYD, *Polymer* **26** (1985) 1123.
12. R. DIAZ-CALLEJA, E. RIANDE and J. SAN ROMAN, *J. Phys. Chem.* **96** (1992) 931.
13. VON O. BROENS and F. H. MÜLLER, *Kolloid Z.* **140** (1955) 121.

Received 9 November 1993
and accepted 24 August 1994